THE GEOLOGICAL SOCIETY OF AMERICA®

Giant deep submarine depressions: A combined dissolution-mechanical process along carbonate margins

T. Mulder[1,†], T. Cavailhes[1], V. Hanquiez[1], H. Gillet[1], A. Recouvreur[1], and N. Fabregas[2]

[1]*Université de Bordeaux (Unité Mixte de Recherche 5805 - Environnements et Paléoenvironnement Océaniques et Continentaux-Observatoire Aquitain des Sciences de l'Univers, Centre national de la recherche scientifique) Allée Geoffroy Saint-Hilaire CS 50023 33615 Pessac, France*

[2]*University of Bergen, Department of Earth Science, Realfagbygget-Allégaten 41, 5020 Bergen, Norway*

ABSTRACT

Submarine depressions are common features on the eastern Bahamian seafloor but the genesis of the deepest ones (>4000 m in water depth) is not well understood. We conducted a morphometric analysis and compared them to a worldwide database of rounded depressions, whatever their genesis is. The deep Bahamian depressions are large elongated structures, among the largest on Earth, with a width greater than 1000 m and a depth sometimes greater than 200 m. They extend at the toe of the Blake Bahama Escarpment (BBE), one of the tallest escarpments on Earth. Some of them align parallel to the BBE. Other depressions align along large submarine canyon axes. When aligned along canyon axes, the depressions closest to the canyon head are flanked by a topographic high interpreted as a slope-break deposit, i.e., sediment deposited after flow expansion following a hydraulic jump. Turbidity currents in the carbonate canyon system are not permanent processes, but are rather triggered during sea-level highstands when the carbonate platform is flooded. In addition, some depressions are not located in canyon axes. Consequently, the size and location of the depressions are not likely explained by a simple plunge pool mechanical erosion. Rather, our data suggest that all depressions could be initiated by giant karstic dissolution structures (dolines or sinkholes). Under interpretation, those located in canyon axes are sporadically refreshed by carbonate-laden turbidity currents. The height of the outsized chutes marking the crossing of the BBE by the canyon mouth generates a hydraulic jump allowing sediment deposition toward the bottom of the depression. Large depressions observed at this location in the Bahamas were the result of an initial dissolution phase related to retreat of the BBE and the more recent sediment-laden flow activity. The depressions orientated along canyon axes facilitated the regressive erosion that formed the canyons. At present, the depressions located at canyon mouths act as regular plunge pools.

†thierry.mulder@u-bordeaux.fr.

INTRODUCTION

Depressions are rounded or ellipsoidal structures with a negative relief that can be related to various landforms with different geneses. Geneses include purely mechanical erosion processes related to potential kinetic energy transfer (plunge pools), sediment collapse due to overpressure and upward fluid motion (pockmarks), and purely dissolution processes (dolines or sinkholes). A plunge pool is a special type of pot hole (Whitaker, 1974) that is cone-shaped, circular to ellipsoidal in a horizontal cross-section, and has fluvial structures that occur at the waterfall toe of immature rivers under the action of swirling flow (Gutiérrez and Gutiérrez, 2016). Plunge pools can be up to 200 m wide and 1–90 m deep (Whitaker, 1974). Plunge pools flanking large headscarps can occur both on Mars and Earth (Lamb et al., 2008), either in onshore or offshore environments, and in various bedrocks including magmatic rocks (e.g., Hawaii; Lamb et al., 2007).

Giant circular plunge pools (diameter ~2 km and depth up to 80 m) with a purely mechanical origin have been described in the Dover Strait, the narrowest part of the English Channel separating Great Britain from continental Europe (Gupta et al., 2017) (Fig. 1). These pools were formed in Cretaceous carbonates and were formed by giant waterfalls created by natural dam breaching due to lake overspill. Consequently, they have a subaerial origin, but they are submerged at present. Similar pools formed by mega-floods have also been described in 45,000 year-old Box Canyon (Idaho, USA) and on Mars (Lamb et al., 2008). Subaerial waterfalls commonly retreat due to undercutting. Toppling in bedrock related to fracturing can also explain the upstream propagation of waterfalls, either on Earth or Mars, without undercutting (Lamb and Dietrich, 2009).

Plunge pools have also been described in submarine environments where they usually occur at the base of the continental slope when the change in slope exceeds 4° (Lee et al., 2002). Tectonically induced breaks of slope are important in leading to an abrupt termination of a canyon (Farre and Ryan, 1985). Such plunge pools located at canyon mouths have been described in a convergent tectonic environment (Makran accretionary prism of the northwest India Ocean; Bourget et al., 2011) (Fig. 1). They may also be associated with an abrupt change in slope (knickpoint). At the slope break located at the toe of the slopes, intense scouring leads to enhanced erosion (Bourget et al., 2011). There, plunge pools are produced either by the decrease in shear stress downslope of hydraulic jumps or by the deposition by sediment-laden density flows downslope of the pool (Lee et al., 2002). They are located downslope of a plunge pool. The latter have been previously studied (Mulder and Alexander, 2001) and called slope-break deposits (SBD). Such deposits that can be interpreted as a type of levee deposit (Bourget et al., 2011) located downslope of the pool have been observed in multiple locations (Lee et al., 2002; Bourget et al., 2011). In addition, sediment waves are frequently observed downslope of the pool, suggesting sediment deposition or remolding by sediment-laden flows (Bourget et al., 2011; Schnyder et al., 2018).

Dissolution by fluid circulation is a typical process in carbonates and in particular in present-day carbonate platforms (Paull et al., 1990). Fluids involved in dissolution processes are

GSA Bulletin; https://doi.org/10.1130/B36142.1; 6 figures.

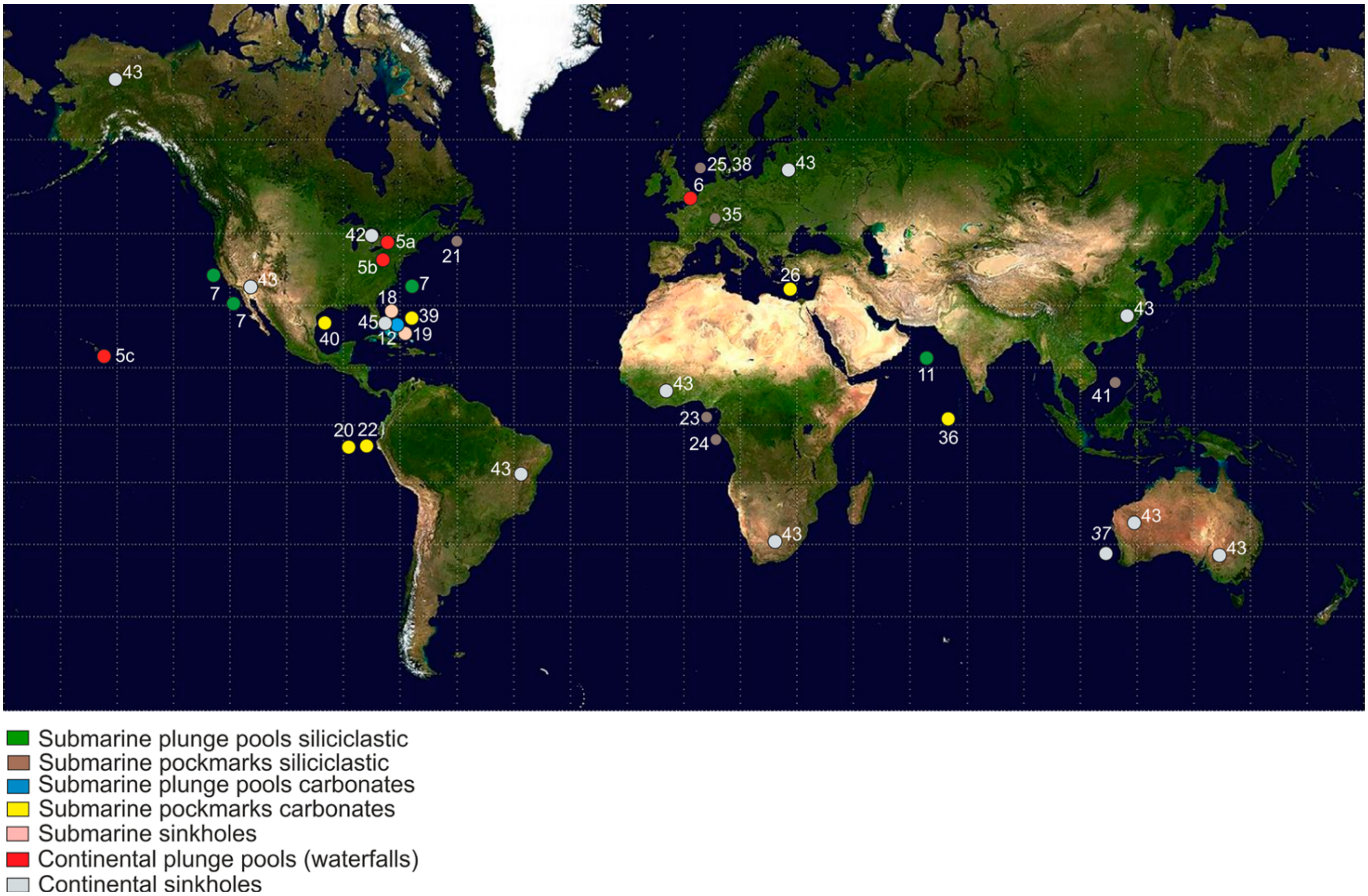

Figure 1. World location of subaerial and submarine rounded depressions studied in this paper. Numbers are referenced in Figure 5 captions.

efficiently directed by structural heterogeneities that form high-permeability structures that drive the dissolving fluid to the surface. Dissolution is emphasized by circulation of saltwater and fresh/saltwater mixing (Kohout convection; Kohout, 1960). Dissolution of anhydrite beds can be responsible for intense under-caving with a rate of horizontal retreat greater than 1 km/m.y. and of only 2 m/m.y. without anhydrite (Paull et al., 1991). In the Bahamian lithologic section, thick restricted marine anhydrites and halites exist and form efficient seals (Walles, 1993). Dredging along the BBE near the Samana re-entrant shows the vertical succession of soft chalk, sometimes rich in organic matter overlain by more indurated deepwater (turbidites) and finally supratidal limestones (Schlager et al., 1984). In a karstic environment, dissolution is responsible for very large and deep collapse depressions with steep sidewalls (close to vertical). These are usually called dolines, sinkholes, or tiankeng in China. In the Bahamas or in Belize, several landforms belong to this category (Mylroie et al., 1995). Sinkholes can be found in the submarine environment (Land et al., 1995; Land and Paull, 2000), however, sinkholes discovered at a water depth of greater than 200 m cannot be explained by classical karstic dissolution, i.e., corrosion by meteoric waters. Deep-sited sinkholes in the Bahamas are related to brine-rich deep-fluid circulation (Paull and Neumann, 1987; Cavailhes et al., 2022). Sinkholes emitting H_2 have been recently discovered in intracratonic basins (banded iron formation; Moretti et al., 2021; Geymond et al., 2022). Similar-sized dissolution structures have been recently discovered on Saturn's largest moon Titan which has a hydrocarbon-dominated atmosphere, suggesting that such dissolution structures exist in extra-terrestrial environments such as on Titan (Cornet et al., 2015) and on Mars (Parenti et al., 2020). These structures are related to evaporate dissolution. In the Mars case, canyon formation by retrogressive erosion is linked to depression alignments.

Pockmarks share morphological similarities with plunge pools or dissolution depressions. They are rounded depressions but are related to escaping sub-bottom fluid that leads to physical excavation (King and MacLean, 1970). They can sometimes be as large as giant plunge pools when they are associated with dissolution processes (Michaud et al., 2005; Sultan et al., 2010) (Fig. 1). Pockmarks on the West African continental margin can reach a diameter of 1000 m and a depth of 100 m (Pilcher and Argent, 2007). Those in the Maldives can reach a diameter of 3000 m and a depth of 180 m (Fig. 1).

It has been previously noted that dissolution combined with unidentified erosional processes were active in giant carbonate canyons (Land et al., 1999). In this paper, we show that multiple processes are necessary for the origin of a giant submarine carbonate canyon and describe the associated submarine morphologies including large depressions bordering the Blake Bahama Escarpment (BBE) in the Eastern Bahamas.

GEOLOGICAL SETTING

The Bahamas represent the most unique siliceous-free carbonate depositional environment in the world. Only a small quantity of wind-driven particles reaches the archipelago. The present-day Bahamas is composed of several

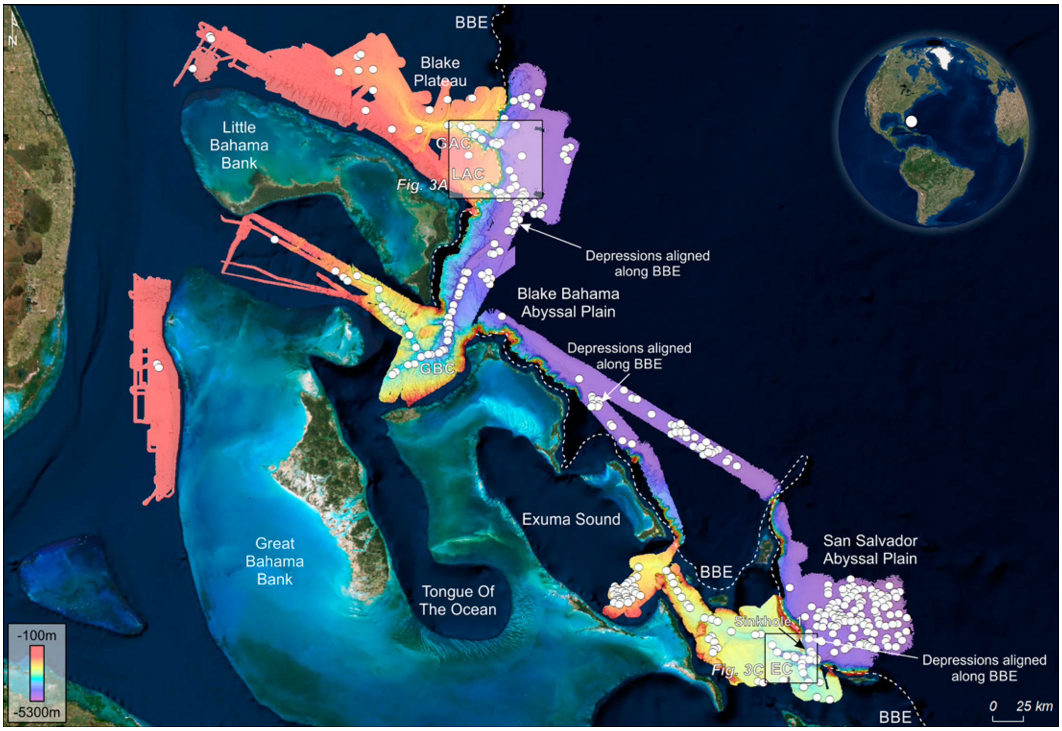

Figure 2. General map of the Bahamian seafloor showing the distribution of deep-seated depressions at the toe of the Blake Bahama Escarpment (BBE). Some are aligned along the BBE, others are in large canyon axes. The depressions located farthest seaward of Exuma Sound could potentially be related to oceanic crust morphologies rather than to carbonate morphologies. Dashed line represents the BBE. White circles represents Bahamian depressions analyzed in this paper. GAC—Great Abaco Canyon; GBC—Great Bahama Canyon; EC—Exuma Canyon; LAC—Little Abaco Canyon.

large carbonate platforms separated by large intrashelf basins and giant submarine canyons usually aligned parallel to platforms (Fig. 2; Mulder et al., 2018, 2019). In the case of the Great Abaco Canyon, the faults are oriented parallel to the canyon suggesting a structural control of canyon orientation (Sheridan et al., 1981, 1988). During the Cenozoic, the platform experienced significant retreat between 5 and 15 km (Freeman-Lynde et al., 1981; Paull and Dillon, 1980; Land et al., 1999). The retreat of the platform created the BBE, a 4 km high submarine topographic features. Relatively small plunge pools in the Bahamas have been described along the western Bahama Bank (Schnyder et al., 2018). These small pools are associated with sediment wave fields. Along this area, the observed depressions are shallow (average water depth of 177 m) and have an average depth of 22 m. They have an ellipsoidal shape with an average width of 211 m and an average length of 283 m. Their inferred formation process is density cascading of dense water at the bank edge. Deep-sea sinkholes have been described along the Florida Escarpment (e.g., water depth of ~450 m, Land and Paull, 2000; ~ -575 m water depth, Land et al., 1995). They were formed by carbonate dissolution under the action of brines circulating inside the drowned platform. Brines are made of sulphides generated by the dissolution of anhydrite sulphates, and their motion is initiated by geothermal heating (Paull and Neumann, 1987; Paull et al., 1990, 1991).

DATASET

Data were acquired during the CARAMBAR and the CARAMBAR 2 cruises (Mulder, 2010, 2017). We also used data provided by the National Oceanic and Atmospheric Administration (NOAA) for areas around the Great Bahama Canyon (UH, 2002; NOAA/AOML, 2002 and 2003; WHOI, 2003 and 2005; NOAA, 2012). The CARAMBAR cruise was conducted from 31 October to 29 November 2010 by *R/V Le Suroît* along the slopes of the Little Bahama and Great Bahama banks. CARAMBAR 2 cruise was conducted from 30 November 2016 to 2 January 2017 by *R/V L'Atalante*, and it recognized the north-eastern slope of the Little Bahama Bank including the Great Abaco and Little Abaco canyons, and the ultra-deep part of the carbonate Bahamian system from the southern part of the Exuma Sound to the San Salvador Abyssal Plain. Onboard equipment during CARAMBAR and CARAMBAR 2 cruises included EM302, EM122, and EM710 multibeam echosounders (Kongsberg Maritime, Horten, Norway), an echo sub-bottom profiler (chirp frequency modulation), a high-resolution 192 channels/fold 24 seismic instrument, and a Kullenberg corer (Mulder, 2010, 2017).

METHODOLOGY

Depression identification and spatial analysis (e.g., map algebra and statistics) were performed using ArcGIS®Desktop v10.5 software. Depressions were automatically identified using the outermost closed isobath of structures with a diameter of at least 1 km (Bauer, 2015; Fig. 2). Manual quality control was carried out in order to invalidate artifacts.

SBD could not be measured automatically because their topographic relief is small relative to the depression, and consequently represent more diffused structures. In addition, SBD are only encountered on depressions located close to the BBE and in canyon axes. The most prominent SBD occurring immediately downslope of the major depressions close to the BBE were manually measured (width, length, and height; Fig. 3B). Their volumes were estimated assuming that they had a conic structure.

During the CARAMBAR 2 cruise, a classical 2.26-m-long Kullenberg core (CAR2KS19) was collected from the deposits (SBD) flanking the most upstream depression of Great Abaco Canyon. The core was located at N 23°19.507, W 74°25.679 at 3860 m water depth. It was globally made of sticky brown mud with calcareous clasts and siliciclastic gravels (Fig. 3D).

RESULTS

A total of 344 depressions have been measured in the study area including the sinkholes in the eastern Bahamas (Cavailhes et al., 2022). Of these, 195 depressions are isolated structures and 149 are coalescent. The depression length varies

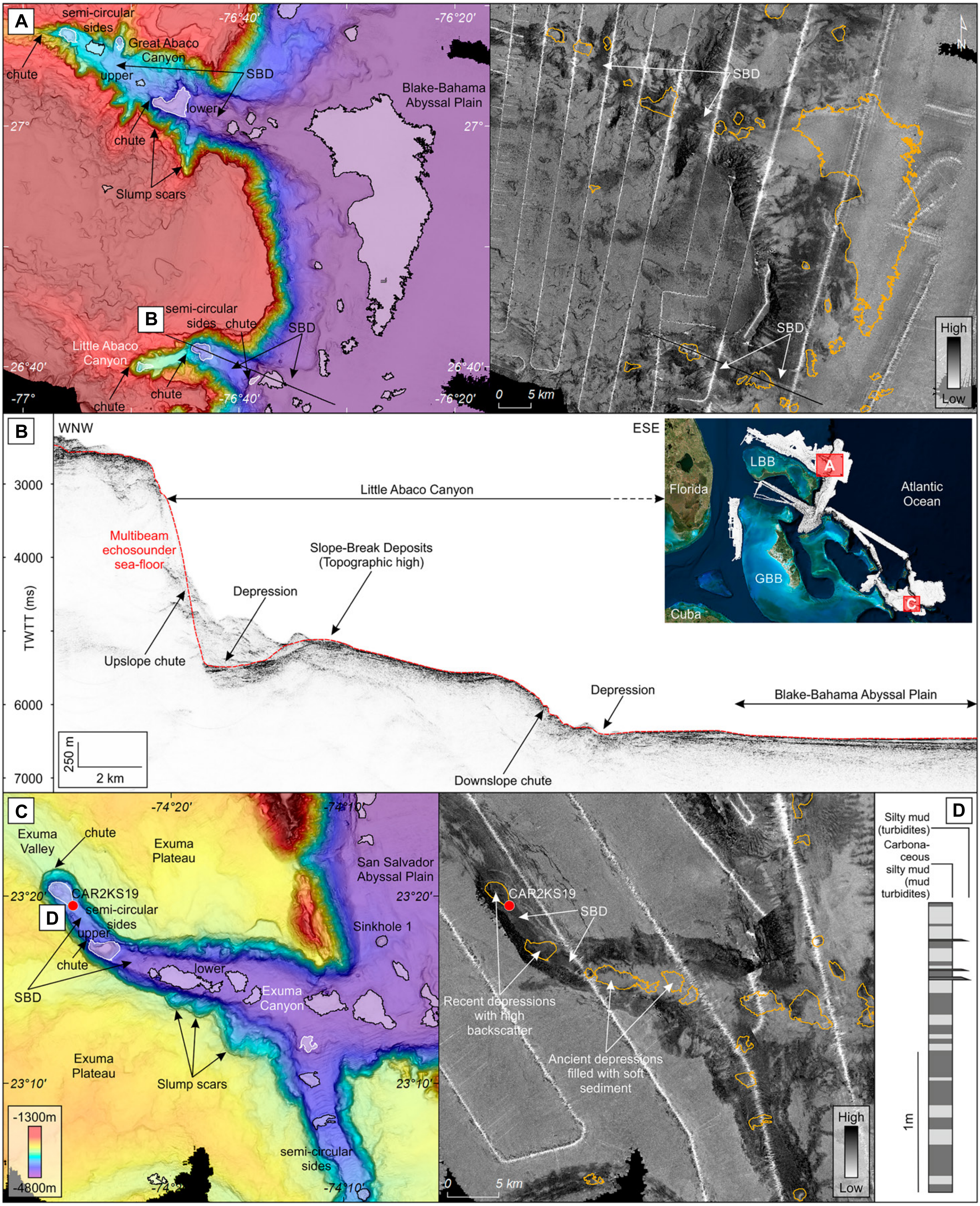
A
semi-circular sides
Great Abaco Canyon
chute
upper
SBD
lower
chute
Slump scars
Blake-Bahama Abyssal Plain
-76°40'
-76°20'
27°
B
semi-circular sides
chute
SBD
Little Abaco Canyon
chute
chute
26°40'
-77°
High
Low
0 5 km
B
WNW
ESE
Little Abaco Canyon
Multibeam echosounder sea-floor
Slope-Break Deposits (Topographic high)
Depression
Upslope chute
Depression
Blake-Bahama Abyssal Plain
Downslope chute
TWTT (ms)
3000
4000
6000
7000
250 m
2 km
Florida
LBB
GBB
Cuba
Atlantic Ocean
A
C
C
Exuma Valley
chute
Exuma Plateau
San Salvador Abyssal Plain
-74°20'
-74°10'
23°20'
CAR2KS19
D
semi-circular sides
upper
chute
SBD
lower
Exuma Canyon
Sinkhole 1
Exuma Plateau
Slump scars
23°10'
semi-circular sides
-1300m
-4800m
CAR2KS19
SBD
Recent depressions with high backscatter
Ancient depressions filled with soft sediment
0 5 km
High
Low
D
Silty mud (turbidites)
Carbonaceous silty mud (mud turbidites)
1m

Figure 3. (A) Bathymetric map and backscatter map at the mouth of Great Abaco Canyon, Northeast Bahamas, Atlantic Ocean. Deepest depressions are white-circled. Other depressions are black circled. (B) Chirp seismic profile showing fault beneath large depressions and slope break deposit (SBD). (C) Bathymetric map and backscatter map showing depressions (black-circled and yellow-circled, respectively) in Exuma Canyon (east of Bahamas, Atlantic Ocean) and at its mouth including the location of core CAR2KS19 (orange circle) collected in the slope break deposits following the most upstream Exuma upper Canyon chute. (D) Core collected in a depression at the mouth of Exuma Canyon, showing three very fine sand carbonate turbidites into a slightly to moderately carbonated mud. TWT—two-way time.

between 1167 and 36,235 m and the depression width varies between 593 and 18,913 m (Fig. 4A). The width versus length graph shows that the shapes of the depressions follow a linear relationship, suggesting that both the coalescent and isolated structures can be merged into the same data group for analysis. Depressions are slightly elongated (elongation factor is defined as length/width is 2.67; Fig. 4A), their surface area varies from 78 to 327 km^2 and their volume ranges from 626×10^{-4} to 5.04 km^3.

The large depressions studied in this work are located both in and out of the axes of giant canyons on the seaward side of the BBE (Figs. 2 and 3). Some of the depressions are aligned along the BBE (Fig. 2) (Cavailhes et al., 2022), others are located in the axis of canyons. Where this is the case, depressions are farther from the BBE. Four canyon areas and their tributaries are included in this study: The Little Abaco Canyon, the Great Abaco Canyon, the Great Bahama Canyon, and the Exuma Canyon. They occur where the submarine valleys cross the BBE. In the Bahamas, canyons that cross the BBE can be subdivided into an upper and lower section, similarly to what Harris et al. (1990) observed along the Florida escarpment. The upper canyon is at a lower bathymetry than the lower canyon and the two section are separated by a chute several hundreds of meters high. The upper canyon is flat floored and cut by a small thalweg (Mulder et al., 2018, 2019) or valley. The presence of this thalweg suggests the activity of sediment-laden gravity flows. Both upper and lower canyons show circular depressions.

When crossing the BBE, canyon profiles show two large chutes, upslope and downslope, flanking the deepest depressions (Fig. 3). Each depression is followed by a topographic high (Fig. 3B). The height of the upslope chutes varies between 78 and 875 m while that of the downslope chutes varies between 554 and 2316 m. Chutes along the BBE are outsized in the submarine environment (Mulder et al., 2018). For example, gully elevation landward of pools ranges from 280 to 700 m (Lee et al., 2002). If the pools have a purely mechanical origin, this value can be used as a proxy for the potential energy of sediment-laden flows. In addition, canyon sides show arcuate or semi-circular sides suggesting that rounded structures precede erosion by slumps.

In this study, some depressions are located immediately downslope of the chute (e.g., Great Abaco and Little Abaco canyons and Exuma Canyon), but they are more frequently located more than three km away from the chute (Great Abaco Canyon) and are aligned along the BBE. Consequently, they are not related to the present-day chutes. In addition, the deepest point of the depression can be located on the side of the chute, not in the canyon axis, which is also not consistent with a direct link with a plunging sediment-laden flow. A direct mechanical erosion necessitates a plunge pool in the flow axis like for a classical waterfall. Consistent with these observations, the height of the chute is not correlated to the depth of the depression. In some cases, for example, Great Abaco and Little Abaco canyons (Fig. 3A), and Exuma Canyon (Fig. 3C) are observed to have successive depressions with similar shapes. Backscatter data show high-amplitude backscatter in the depressions. This suggests presence of coarse or indurated sediment filling the depression, similar to the strong bottom echo at 3.5 kHz observed in the Makran depressions (Bourget et al., 2011). These depressions are close to the BBE. Conversely, in some cases, depressions show low backscatter suggesting recent sediment infilling; These depressions are farther from the BBE. The upper part of the chute and the side of the canyon bordering the depression show numerous arcuate structures interpreted as slump scars.

SBD are located immediately downslope of major depressions (Fig. 3B). The estimated volume of SBD correlates to the volume of the large depressions (Fig. 4B) that adjoin major chutes in the canyons but SBD volume is only 1:100 of the depression volume (Fig. 4B). The core collected from the deposits of the most upstream Great Abaco Canyon depression used in the study had a tube length of 5 m and the obtained core was 2.2 m long. During coring, the tube was twisted, suggesting that the thickness of the soft deposit was not important. The sediment shows poorly sorted carbonate mud with numerous lithoclasts caused by seafloor erosion (Fig. 3D). Three thin, very fine-grained, and sandy carbonate turbidites were found intercalated between the poorly sorted mud, indicating sporadic deposition by sediment-laden flows. The presence of SBD containing gravity-flow deposits immediately downslope of the depression suggests that mechanical processes are active at the depression location. The shape of the SBD and the collected deposits are similar to that obtained through the numerical modeling of SBD (Lee et al., 2002). The flow excavates the initial depression and

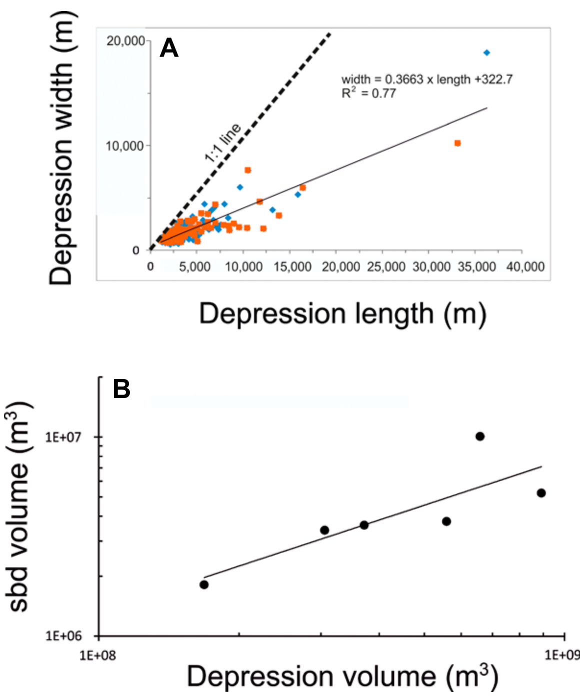

Figure 4. (A) Width versus length of the 344 isolated (blue diamonds) and coalescent (red squares) depressions of the present study (all located east of the Bahamas, Atlantic Ocean). (B) Slope break deposit (SBD) volume versus depression volume. Note that SBD volume is 1:100 of depression volume. Number of measurements of SBD is small because SBD are only observed on the youngest depressions close to the BBE.

the eroded material is deposited downslope. However, despite correlated to the volume of the depression, the volume of the SBD is very small. An explanation of the missing volume (99%) is that the main process explaining the size of the depression may not directly relate to sediment-laden flow processes. In addition, as some depressions are located along the BBE but not in the axis of canyons or smaller submarine valleys, this suggests that the depression initiation is not mechanical. Consistently, the deepest point of depression is sometimes on the side of the depression floor and not in the axis of the potential plunging flow. Consequently, mechanical erosion appears to be only an additional process for depressions located in canyon axis.

The Bahamian depressions are outsized because of their combined depth and width. Figure 5 shows that the Bahamian depressions are among the largest in width when compared with other the rounded depressions on Earth (Fig. 1), including the giant pockmarks on the west African margin (Pilcher and Argent, 2007), the plunge pools and pockmarks in siliciclastic environments (Lee et al., 2002; Sultan et al., 2010; Cole et al., 2000), and the giant dissolution structure in a mixed oceanic ridge-carbonate drape (Michaud et al., 2005). They are also larger than the plunge pools of the Dover Strait that were formed by a lake outburst in a subaerial environment (Gupta et al., 2017). The Bahamian depressions are also as large as or even larger than all subaerial structures including dissolution mega-dolines and classical waterfall-related plunge pools. Only the largest terrestrial meteoric-water related megadolines are deeper than the Bahamian depressions for an equivalent diameter.

DISCUSSION

Most papers that have dealt with such submarine depressions interpreted them as plunge pools (Gupta et al., 2017; Lee et al., 2002; Bourget et al., 2011; Schnyder et al., 2018), that is, the depression is located immediately downslope of the chute, which is consistent with mechanical erosion. The remaining papers interpret them as pockmarks (King and MacLean, 1970; MacDonald et al., 1990; Cole et al., 2000; Betzler et al., 2011; Hovland et al., 2005; Pilcher and Argent, 2007; Sultan et al., 2010). The location of the pool just down a valley marks a significant difference in the characteristics of the Bahamian depressions. Some are downslope of the valley but a large amount of depressions are dissociated from valleys. In most cases, there is a large distance between the valley, the chutes, and the depressions suggesting the relatively minor role of mechanical erosion in initiating the depressions. However, the largest depressions are the closest to the chute suggesting the mechanical impact is not negligible.

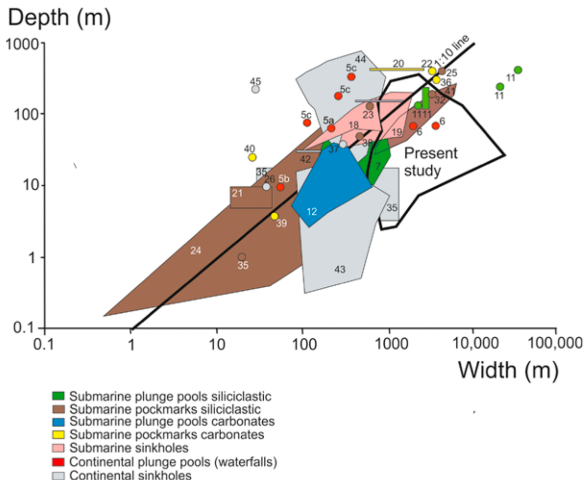

Figure 5. (A) Depth versus width of selected representative subaerial and submarine depressions worldwide. Data from (A) Niagara Falls, USA, (B) Taughannock Falls, USA, (C) Hawaii, Homokane Valley; subaerial dolines (5); Gupta et al., 2017 (6); Lee et al., 2002 (7); Bourget et al. (2011) (11); Schnyder et al., 2018 (12); Land and Paull, 2000 (18); Cavailhes et al., 2022 (19); Michaud et al., 2018 (20), King and MacLean, 1970 (21); Michaud et al., 2005 (22); Sultan et al., 2010 (23); Pilcher and Argent, 2007 (24); Cole et al., 2000 (25); Mitchell et al., 2013, Erasthostene seamount (26); Chapron et al., 2004 (27); Parenti et al., Mars, 2020 (35); Betzler et al., 2011 (36); Backshall et al., 1979, Blue Holes–Great Barrier, Australia (37); Hovland et al., 2005 (38); Paull et al., 1996 (39); MacDonald et al., 1990 (40); Zhang et al., 2020 (41); Ruberg et al., 2008, Lake Huron, North America (42); Moretti et al., 2021; Geymond et al., 2022, banded iron formation (43); this is number 5: moved upside; subaerial doline morphometry https://fr.wikipedia.org/wiki/Liste_des_méga-dolines(44). Dean's Blue Hole, Bahamas (45). For references presenting a cloud of dots, only extreme values are plotted to generate the cloud envelope.

Figure 5 shows the depth versus width plot for a large published data set of subcircular natural depressions in the world. All the points scatter around a line in the log-log graph indicating that the depth:width of the depression is constant irrespective of the nature of the depression (pockmark, plunge pool, and sinkholes), environment (subaerial or submarine), and lithology (siliciclastic, carbonate, and volcanic). This represents the mean slope between the edge and the middle of the depression. The asymmetry is 2.73, slightly higher than values published by Land and Paull (2000) (1.1–2.15).

These observations strongly suggest that sporadic sediment-laden flow cannot be the only origin of such large depressions and that depressions are anterior to the sediment-laden flows. In addition, the spatial distribution of depressions (Fig. 3A) suggests that they are not strictly related to the present-day chutes. The deepest present-day depressions are located close to the chutes (Fig. 3), but other well expressed depressions are away from the chutes and sometimes at the edge of the abyssal plain (Fig. 2; Cavailhes et al., 2022). However, the presence of SBD proves that sporadic sediment-laden flows are driven into the depressions when the depressions are located in a valley.

Orientations of canyons along structural lineaments (Cavailhes et al., 2022) suggest that backstepping erosion followed these weak zones during the retreat of the BBE and oriented the canyons parallel to the bank's margin (Paull and Dillon, 1980). In addition, depressions are located at the intersection of canyons and faults. Field evidence suggests that mesh structures including faults form important conduits for the flow of a large volume of hydrothermal fluids (Sibson, 1996). A strong directional permeability develops in the direction parallel to fault-fracture intersections. These fault intersections (structural permeability) would therefore drain the saline brines, aided by thermal convection. The presence of pre-existing faults suggests that sulphide-rich fluids can be driven to the surface along structural weaknesses and that depression formation could be initiated in a similar way as sinkholes (Cavailhes et al., 2022). In addition, semi-circular sides of canyons suggest that canyon erosion rooted on depressions. No depression is observed on the shelf suggesting that depressions developing upside of a canyon head are buried and form by hypogenic processes.

The analysis of giant depressions in the Bahamas presented in this paper supports an original five-phase hypothetical formation model and several processes. Steepness and morphology of the canyon walls both suggest that unidentified erosional processes occurred at the canyon heads in addition to dissolution. The first phase represents the initial location of the BBE. Early canyon erosion occurred along structural lineaments and related depressions. Dashed circles upward in the canyon heads suggest that subbottom depressions were formed by hypogenic dissolution along lineaments and orientate canyon backward erosion. (Fig. 6A). The second phase was marked by intensified focused dissolution. Brines moved toward the lowest point of the system (growing canyon) due to their relative high density compared to

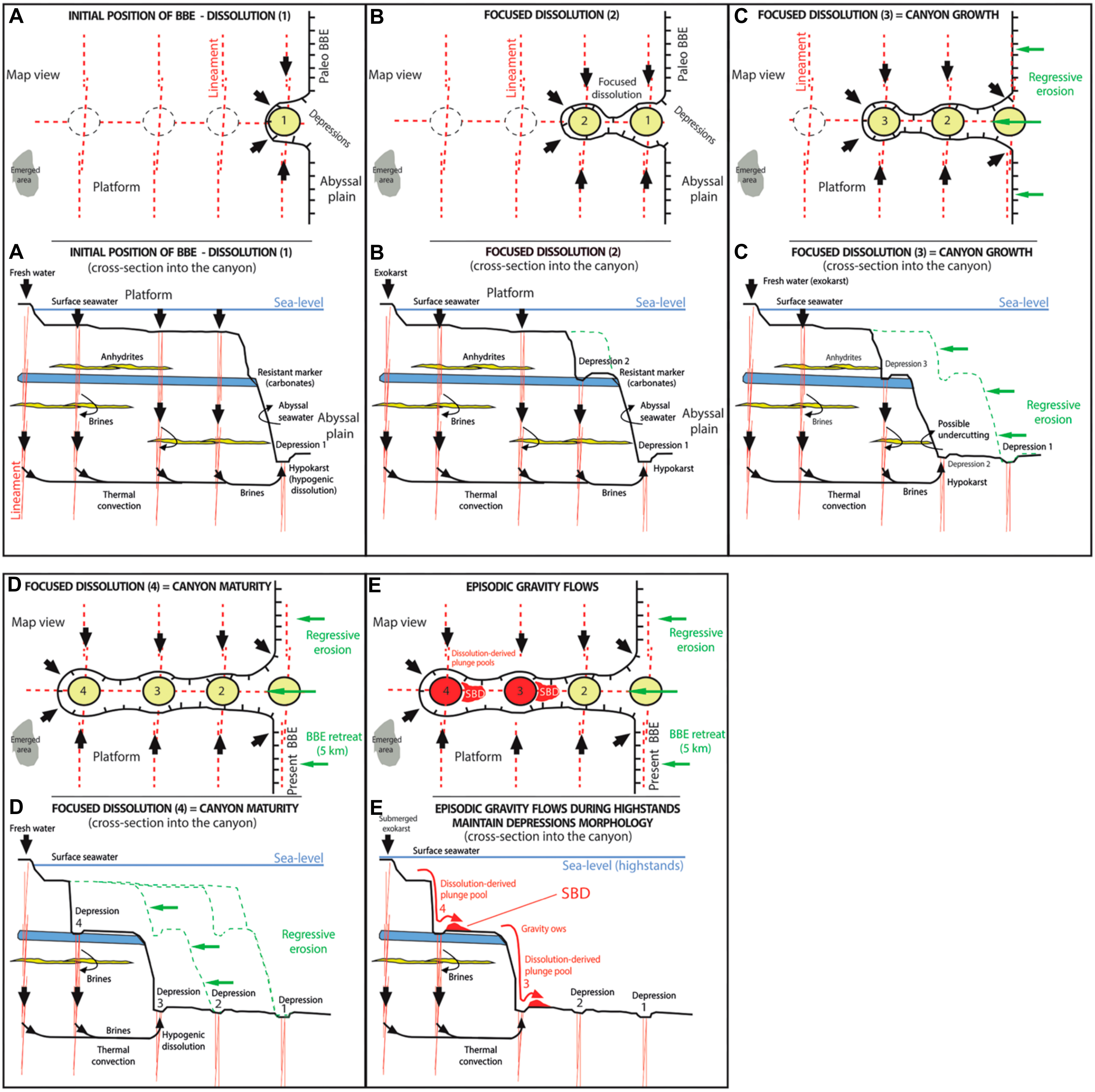

Figure 6. Synthetic sketch showing the five steps in the formation of depressions. For each step, there is a map view and a cross-section into the canyon. Figure not to scale. (A) Initial position of the Blake Bahama Escarpment (BBE) and early dissolution. (B) Focused dissolution begins by brine circulation along faults during Cretaceous. (C) Focused dissolution and canyon growth by retrogressive erosion (D) Backward erosion stabilization and canyon maturity phase. (E) Present-day state with sporadic turbidity currents using the depressions as plunge pools. SBD—slope-break deposits.

seawater, preferentially along the structural heterogeneities. BBE retreat began during Late Cretaceous and early Cenozoic. Erosion could thus be partly driven by the presence of resistant carbonate levels. This retreat signifies the start of undercutting related to the initiation of dissolution by brine motion under the action of thermal heat, brine-hydraulic-head gradient, and Kohout convection. Brine motion was still driven along the faults. This phase is supposed to be related to brine circulation along with the increase in heat flow (Fig. 6B). Brines generated from evaporites first flew downward, and then upward along faults and fractures (Chanton et al., 1991). Fluids escaped through surface-created dissolution depressions with a steep angle (close to vertical) that are similar to that in hypogenic dolines. During the third phase, hypogenic dissolution and BBE retreat intensified. Chutes progressively retreated from the edge of the BBE to form the present-day canyons (Fig. 6C). This phase represents the most intense period of retrogressive erosion. Undercutting based on the levels where anhydrites occurred probably played a major role in directing and enhancing retrogressive erosion (Paull and Neumann, 1987; Chanton et al., 1991). At present day, canyons are aligned along depressions and have semi-circular edges enhanced by slumping. Oldest outcropping depressions are far from the canyon head while recently outcropping depressions are close to the canyon head. In other words, the formation of dissolution structures controls the direction of retrogressive erosion. Consequently, the canyon mouth moved from the initial BBE edge to its present-day location. The fourth stage represents the mature phase of a canyon (Fig. 6D). Regressive erosion decreases and canyon morphology stabilized. Total BBE retreat comprises between 5 and 15 km (Paull and Dillon 1980; Freeman-Lynde at al., 1981, Freeman-Lynde, 1983, Dillon et al., 1987). Backward erosion still occurred along areas of weakness defined by both structural lineaments and dissolution structures. Formation of re-entrant and large canyons began during this phase. Failure scars indicate initial erosion in this phase and the semi-circular morphology of the canyon side suggests that canyon erosion rooted on depressions. Steps in the chute are related to the lithologically hard layers (Fig. 6D).

Phase five represents the present-day status (Fig. 6E) (Lamb et al., 2008). Sediment-laden flows are channeled by canyons or valleys and contribute to maintaining the freshness of the morphology of the canyon and depressions. In such depressions, flows experience enhanced turbulence (hydraulic jump) and the resulting deposits are well-sorted sediments in the size range of fine sand to silt. Excavation and sediment laden flows would thus be sporadic (during highstands) whereas the dissolution process would be continuous as suggested by the freshness of the depressions that have been recognized out of the canyon axes. Dissolution might be enhanced during sea-level lowstands because of the reactivation of the exokarstic system. Either flow inertia or the formation of hydraulic jumps contributed to the formation of SBD. A deeper depression leads to a higher turbid cloud resulting from the jump, and consequently, a thicker SBD. Considering the depth of the depression, erosion rate within it is probably low because the turbulent flow encounters lithified rocks rather than soft sediments. A part of the SBD is deposited downslope of the depression, but when the height of the SBD is sufficient, the deposit progrades toward the depression. The bottom of the depressions is thus progressively filled by deposits, reducing the depression depth.

Our work can be placed in worldwide literature on large depressions: Three groups of depressions were identified in the literature: (1) Purely karstic sinkholes formed by carbonate dissolution during the emergence of the carbonate platform. These are usually submerged at present in shallow waters (<120 m water depth) and were included in this study for the comparison of structures. (2) Brine-related dissolution depressions that form the present-day sinkholes. These are concentrated at the toe of the BBE and have been extensively studied. (3) Sinkhole-derived plunge-pools. Plunge pools can be either active or inactive, and mechanical erosion maintains the freshness of these depressions. In all cases, dissolution seems to be the prominent mechanism that initiates the depression.

CONCLUSIONS

In this study, we performed a morphometric analysis of giant depressions located in eastern Bahamas, either at the toe of the BBE, or across the BBE, in the axes of canyons. When they are in canyon axes, they usually form alignments. The depression closest to the canyon head is flanked with SBD. When they are not in a canyon axis, they may be aligned along the BBE. Comparison of these submarine depressions with worldwide, subaerial and submarine depressions shows they are among the largest on Earth. The results suggest that Bahamian depressions are firstly formed by underwater carbonate dissolution just after BBE retreat and later used as plunge pools thus experiencing mechanical erosion. As dissolution is related to the upward drainage of brines (hypogenic karstification), tectonic control by structural lineaments is also important for explaining the genesis of a depression. Brine-related dissolution depressions and sinkhole-derived plunge-pools are deep structures that can be observed up to a water depth of 5000 m along one of the steepest large-scale landforms on Earth. Submarine depressions in the Bahamas are complex structures belonging to sinkhole-derived plunge-pools. They play an important role in shaping submarine geomorphology and box-shape canyons. In the Bahamian case, they orientate canyon direction by controlling retrogressive erosion.

ACKNOWLEDGMENTS

We thank the captain and crew of the *R/V L'Atalante* for the quality of the acquired data and Ifremer-Genavir for cruise organization and technical support during cruise CARAMBAR 2. We thank Dr. Chris Sheehan and Dr. Ángel Puga Bernabéu for their constructive reviews of the early version of the manuscript.

REFERENCES CITED

Backshall, D.G., Barnett, J., Davies, P.J., Duncan, D.C., Harvey, N., Hopley, D., Isdale, P.J., Jennings, J.N., and Moss, R., 1979, Drowned dolines: The blue holes of the Pompey Reefs, Great Barrier Reef: BMR Journal of Australian Geology and Geophysics, v. 4, p. 99–109.

Bauer, C., 2015, Analyse of dolines using multiple methods applied to airborne laser scanning data: Geomorphology, v. 250, p. 78–88, https://doi.org/10.1016/j.geomorph.2015.08.015.

Betzler, C., Lindhorst, S., Hubscher, C., Ludmann, T., Furstenau, J., and Reijmer, J., 2011, Giant pockmarks in a carbonate platform (Maldives, Indian Ocean): Marine Geology, v. 289, p. 1–16, https://doi.org/10.1016/j.margeo.2011.09.004.

Bourget, J., Zaragosi, S., Ellouz-Zimmermann, N., Mouchot, N., Garlan, T., Schneider, J.-L., Lanfumey, V., and Lallemant, S., 2011, Turbidite system architecture and sedimentary processes along topographically complex slopes: The Makran convergent margin: Sedimentology, v. 58, p. 376–406, https://doi.org/10.1111/j.1365-3091.2010.01168.x.

Cavailhes, T., Gillet, H., Guiastrennec-Faugas, L., Mulder, T., and Hanquiez, V., 2022, The abyssal giant sinkholes of the Black Bahama Escarpment: Evidence of focused deep-ocean carbonate dissolution: Geomorphology, v. 398, https://doi.org/10.1016/j.geomorph.2021.108058.

Chanton, J.P., Martens, C.S., and Paull, C.K., 1991, Control of pore-water chemistry at the base of the Florida escarpment by processes within the platform: Nature, v. 349, p. 229–231, https://doi.org/10.1038/349229a0.

Chapron, E., Van Rensbergen, P., De Batist, M., Beck, C., and Henriet, J.-P., 2004, Fluid-escape features as a precursor of a large sublacustrine sediment slide in Lake Le Bourget, NW Alps, France: Terra Nova, v. 16, p. 305–311, https://doi.org/10.1111/j.1365-3121.2004.00566.x.

Cole, D., Stewart, S.A., and Cartwright, J.A., 2000, Giant irregular pockmark craters in the Palaeogene of the Outer Moray Firth Basin, UK North Sea: Marine and Petroleum Geology, v. 17, p. 563–577, https://doi.org/10.1016/S0264-8172(00)00013-1.

Cornet, T., Cordier, D., Le Bahers, T., Bourgeois, O., Fleurant, C., Le Mouélic, S., and Altobelli, N., 2015, Dissolution on Titan and on Earth: Toward the age of Titan's karstic landscapes: Journal of Geophysical Research. Planets, v. 120, p. 1044–1074, https://doi.org/10.1002/2014JE004738.

Dillon, V.P., Valentine, P.C., and Paull, C.K., 1987. The Blake Escarpment: A product of erosional processes in the deep ocean, *in* Cooper, R., and Shepard, A.N., eds., Scientific Application of Current Diving Technology on the U.S. Continental Shelf: U.S. Department of Commerce, Symposium Series for Undersea Research, v. 2, p. 177–190.

Farre, J.A., and Ryan, W.B.F., 1985, 3-D view of erosional scars on U.S. mid-Atlantic continental margin: The American Association of Petroleum Geologists Bulletin, v. 69, p. 923–932.

Freeman-Lynde, R.P., 1983, Cretaceous and Tertiary samples dredge from the Florida Escarpment, Eastern Gulf of Mexico: Transactions-Gulf Coast Association of Geological Societies, v. 33, p. 91–99.

Freeman-Lynde, R.P., Cita, M.B., Jadoul, F., Miller, E.L., and Ryan, W.B.F., 1981, Marine geology of the Bahama escarpment: Marine Geology, v. 44, p. 119–156, https://doi.org/10.1016/0025-3227(81)90115-8.

Geymond, U., Ramanaidou, E., Lévy, D., Ouaya, A., and Moretti, I., 2022, Can weathering of banded iron formation generate natural hydrogen? Evidence from Australia, Brazil and South Africa: Minerals (Basel), v. 2, no. 12, https:doi.org/10.3390/min12020163.

Gupta, S., Collier, J.S., Garcia-Moreno, D., Oggioni, F., Trentesaux, A., Vanneste, K., De Batist, M., Camelbeeck, T., Potter, G., Van Vliet-Lanoë, B., and Arthur, J.C.R., 2017, Two-stage opening of the Dover Strait and the origin of island Britain: Nature Communications, v. 8, https://doi.org/10.1038/ncomms15101.

Gutiérrez, F., and Gutiérrez, M., 2016, Landforms on Earth: An illustrated Guide: Cham, Switzerland, Springer International Publishing, 270 p., https://doi.org/10.1007/978-3-319-26947-4.

Hovland, M., Svensenb, H., Forsberg, C.F., Johansend, H., Fichlere, C., Fosså, J.H., Jonssong, R., and Rueslåttene, H., 2005, Complex pockmarks with carbonate-ridges off mid-Norway: Products of sediment degassing: Marine Geology, v. 218, p. 191–206.

King, L.H., and MacLean, B., 1970, Pockmarks on the Scotian Shelf: Geological Society of America Bulletin, v. 81, p. 3141–3148, https://doi.org/10.1130/0016-7606(1970)81[3141:POTSS]2.0.CO;2.

Kohout, F.A., 1960, Cyclic flow of salt water in the Biscayne aquifer of south-eastern Florida: Journal of Geophysical Research, v. 65, p. 2133–2141, https://doi.org/10.1029/JZ065i007p02133.

Lamb, M.P., and Dietrich, W.E., 2009, The persistence of waterfall in fractured rocks: Geological Society of America Bulletin, v. 121, no. 7-8, p. 1123–1134, https://doi.org/10.1130/B26482.1.

Lamb, M.P., Howard, A.D., Dietrich, W.E., and Taylor Perron, J., 2007, Formation of amphitheater-headed valleys by waterfall erosion after large-scale slumping of Hawai'i: Geological Society of America Bulletin, v. 119, no. 7-8, p. 805–822, https://doi.org/10.1130/B25986.1.

Lamb, M.P., Dietrich, E.D., Aciego, S.M., DePaolo, J., and Manga, M., 2008, Formation of Box Canyon, Idaho, by megaflood: Implications for seepage erosion on Earth and Mars: Science, v. 320, p. 1067–1070, https://doi.org/10.1126/science.1156630.

Land, L.A., and Paull, C.K., 2000, Submarine karst belt rimming the continental slope in the Strait of Florida: Geo-Marine Letters, v. 20, p. 123–132, https://doi.org/10.1007/s003670000041.

Land, L.A., Paull, C.K., and Hobson, B., 1995, Genesis of a submarine sinkhole without subaerial exposure: Strait of Florida: Geology, v. 23, no. 10, p. 949–951, https://doi.org/10.1130/0091-7613(1995)023<0949:GOASSW>2.3.CO;2.

Land, L.A., Paull, C.K., and Spiess, F.N., 1999, Abyssal erosion and scarp retreat: Deep tow observation of the Blake Escarpment and Blake Spur: Marine Geology, v. 160, p. 63–83, https://doi.org/10.1016/S0025-3227(99)00012-2.

Lee, S.E., Talling, P.J., Ernst, G.G.J., and Hogg, A.J., 2002, Occurrence and origin of submarine plunge pools at the base of the US continental slope: Marine Geology, v. 185, p. 363–377, https://doi.org/10.1016/S0025-3227(01)00298-5.

MacDonald, I.R., Reilly, J.F., Guinasso, J.N.L., Brooks, J.M., Carney, R.S., Bryant, W.A., and Bright, T.J., 1990, Chemosynthetic mussels at a brine-filled 30 pockmark in the northern: Gulf of Mexico Science, v. 248, p. 1096–1099, https://doi.org/10.1126/science.248.4959.1096.

Michaud, F., Chabert, A., Collot, J.-Y., Sallarès, V., Flueh, E.R., Charvis, P., Graindorge, D., Gustcher, M.-A., and Billas, J., 2005, Fields of multi-kilometer scale sub-circular depressions in the Carnegie Ridge sedimentary blanket: Effect of underwater carbonate dissolution: Marine Geology, v. 216, p. 205–219, https://doi.org/10.1016/j.margeo.2005.01.003.

Michaud, F., Collot, J. Y., Ratzov, G., Proust, J. N., Dano, A., Lebrun, J. F., rt al., 2018, A honeycomb seafloor morphology in carbonate sediment of the Carnegie Ridge (offshore Ecuador): Formation and potential geodynamic significance: Geology, v. 46, no. 11, p. 979–982, https://doi.org/10.1130/G45285.1.

Mitchell, G., Mayer, L.A., Bell, K.L.C., Raineault, N.A., and Roman, C., 2013, Exploration of Eratosthenes Seamount–A continental fragment being forced down an oceanic trench, *in* Bell, K.L.C., and Brennan, M.L., eds., New Frontiers in Ocean Exploration: The E/V Nautilus 2012 Field Season and Summary of Mediterranean Exploration: Oceanography, v. 26, no. 1, supplement, p. 36–41.

Moretti, I., Brouilly, E., Loiseau, K., Prinzhofer, A. and Deville, E., 2021, Hydrogen emanations in intracratonic areas: New Guide lines for early exploration basin Screening: Geosciences, v. 11, no. 3, https://doi.org/10.3390/geosciences11030145.

Mulder, T., 2010, CARAMBAR cruise, RV Le Suroît, https://doi.org/10.17600/10020080.

Mulder T., 2017, CARAMBAR 2 cruise, RV L'Atalante, https://doi.org/10.17600/16001500.

Mulder, T., and Alexander, J., 2001, Abrupt change in slope causes variation in the deposit thickness of concentrated particle-driven density currents: Marine Geology, v. 175, p. 221–235, https://doi.org/10.1016/S0025-3227(01)00114-1.

Mulder, T., Gillet, H., Hanquiez, V., Ducassou, E., Fauquembergue, K., Principaud, M., Conesa, G., Le Goff, J., Ragusa, J., Bashah, S., Bujan, S., Reijmer, J.J.G., Cavailhes, T., Droxler, A.W., Blank, D.G., Guiastrennec, L., Fabregas, N., Recouvreur, A., and Seibert, C., 2018, Carbonate slope morphology revealing a giant submarine canyon (Little Bahama Bank, Bahamas): Geology, v. 46, no. 1, p. 31–34, https://doi.org/10.1130/G39527.1.

Mulder, T., Gillet, H., Hanquiez, V., Reijmer, J.J.G., Droxler, A.W., Recouvreur, A., Cavailhes, T., Fauquembergue, K., Blank, D.G., Guiastrennec, L., Fabregas, N., Seibert, C., Bashah, S., Bujan, S., Ducassou, E., Principaud, M., Conesa, G., Le Goff, J., Ragusa, J., Busson, J., and Borgomano, J., 2019, Into the deep: A coarse-grained carbonate turbidite talweg generated by gigantic submarine chutes: Marine Geology, v. 407, p. 316–333, https://doi.org/10.1016/j.margeo.2018.11.003.

Mylroie, J.E., Carew, J.L., and Moore, A.I., 1995, Blue holes: Definition and genesis: Carbonates and Evaporites, v. 10, no. 2, p. 225–233, https://doi.org/10.1007/BF03175407.

National Oceanic and Atmospheric Administration (NOAA/AOML), 2002, Multibeam collection for RB0204: Multibeam data collected aboard NOAA Ship RONALD H. BROWN (R104) from 17-Jun-02 to 29-Jun-02, Jacksonville, Florida to Miami, Florida: NOAA National Centers for Environmental Information, https://www.ngdc.noaa.gov/ships/ronald_h_brown/RB0204_mb.html (accessed 16 January 2018).

National Oceanic and Atmospheric Administration (NOAA/AOML), 2003, Multibeam collection for RB0301: Multibeam data collected aboard NOAA Ship RONALD H. BROWN (R104) from 04-Feb-03 to 15-Feb-03, Charleston, South Carolina to Miami, Florida: NOAA National Centers for Environmental Information, https://www.ngdc.noaa.gov/ships/ronald_h_brown/RB0301_mb.html (accessed 16 January 2018).

National Oceanic and Atmospheric Administration (NOAA), 2012, Multibeam collection for RB1201: Multibeam data collected aboard NOAA Ship RONALD H. BROWN (R104) from 18-Feb-12 to 03-Mar-12, Charleston, South Carolina to Charleston, South Carolina: NOAA National Centers for Environmental Information, https://www.ngdc.noaa.gov/ships/ronald_h_brown/RB1201_mb.html (accessed 16 January 2018).

Parenti, C., Gutiérrez, F., Baioni, D., García-Arnay, Á., Sevil, J., and Luzzi, E., 2020, Closed depressions in Kotido crater, Arabia terra, Mars. Possible evidence of evaporate dissolution-induced subsidence: Icarus, v. 341, https://doi.org/10.1016/j.icarus.2020.113680.

Paull, C., and Neumann, A.C., 1987, Continental margin brine seeps: Their geological consequences: Geology, v.15, p. 545–548.

Paull, C.K., and Dillon, W.P., 1980, Erosional origin of the Blake Escarpment: An alternative hypothesis: Geology, v. 8, p. 538–542, https://doi.org/10.1130/0091-7613(1980)8<538:EOOTBE>2.0.CO;2.

Paull, C.K., Commeau, R.F., Curray, J.R., and Neumann, A.C., 1991, Seabed measurements of modern corrosion rates on Florida Escarpment: Geo-Marine Letters, v. 11, p. 16–22, https://doi.org/10.1007/BF02431050.

Paull, C.K., Spiess, F.N., Curray, J.R., and Twitchell, D.C., 1990, Origin of Florida Canyon and the role of spring sapping on the formation of submarine box canyons: Geological Society of America Bulletin, v. 102, no. 4, p. 502–515, https://doi.org/10.1130/0016-7606(1990)102<0502:OOFCAT>2.3.CO;2.

Paull, C.K., Buelow, W.J., Ussler, W., III, and Borowski, W.S., 1996, Increased continental-margin slumping frequency during sea-level lowstands above gas hydrate-bearing sediments: Geology, v. 24, p. 143–146, https://doi.org/10.1130/0091-7613(1996)024<0143:ICMSFD>2.3.CO;2.

Pilcher, R., and Argent, J., 2007, Mega-pockmarks and linear pockmarks trains on the West African continental margin: Marine Geology, v. 244, p. 15–32, https://doi.org/10.1016/j.margeo.2007.05.002.

Ruberg, S.A., Kendall, S.T., Biddanda, B.A., Black, T., Nold, S.C., Lusardy, W.R., Green, R., Casserley, T., Smith, E., Garrison Sanders, T., Lang, G.A., and Constant, S.A., 2008, Observations of the Middle Island sinkholes in Lake Huron: A unique hydrogeologic and glacial creation of 400 Million Years: Marine Technology Society Journal, v. 42, no. 4, p. 12–21, https://doi.org/10.4031/002533208787157633.

Schlager, W., Austin, J.A., Jr., Corso, W., McNulty, C.L., Fluegel, E., Renz, O., and Steinmetz, J.C., 1984, Early Cretaceous platform re-entrant and escarpment erosion in the Bahamas: Geology, v. 12, p. 147–150, https://doi.org/10.1130/0091-7613(1984)12<147:ECPRAE>2.0.CO;2.

Schnyder, J.S.D., Eberli, G.P., Betzler, C., Wunsch, M., Lindhorst, S., Schiebel, L., Mulder, T., and Ducassou, E., 2018, Morphometric analysis of plunge pools and sediment wave fields along western Great Bahama Bank: Geology, v. 397, p. 15–28, https://doi.org/10.1016/j.margeo.2017.11.020.

Sheridan, R.E., Crosby, J.T., Bryan, G.M., and Stoffa, P.L., 1981, Stratigraphy and structure of southern Blake Plateau, northern Florida Straits, and northern Bahama Platform from multichannel seismic reflection data: AAPG Bulletin, v. 65, p. 2571–2593.

Sheridan, R.E., Mullins, H.T., Austin, J.J.A., Ball, M.M., and Ladd, J.W., 1988, Geology and geophysics of the Bahamas, *in* Sheridan, R.E., and Grow, J.A., eds., The Atlantic Continental Margin: Boulder, Colorado, Geological Society of America, Geology of North America, v. I-2, https://doi.org/10.1130/DNAG-GNA-I2.329.

Sibson, R., 1996, Structural permeability of fluid-driven fault-fracture meshes: Journal of Structural Geology, v. 18, no. 8, p. 1031–1042, https://doi.org/10.1016/0191-8141(96)00032-6.

Sultan, N., Marsset, B., Ker, S., Marsset, T., Voisset, M., Vernant, A.M., Bayon, G., Cauquil, E., Adamy, J., Colliat, J.L., and Drapeau, D., 2010, Hydrate dissolution as a potential mechanism for pockmark formation in the Niger Delta: Journal of Geophysical Research. Solid Earth, v. 115, no. B8, https://doi.org/10.1029/2010JB007453.

University of Hawaii (UH), 2002, Multibeam collection for KM0201: Multibeam data collected aboard Kilo Moana from 25-Jul-02 to 13-Aug-02, Jacksonville, Florida to Balboa, Panama: NOAA National Centers for Environmental Information, https://www.ngdc.noaa.gov/ships/kilo_moana/KM0201_mb.html (accessed 16 January 2018).

Walles, F.E., 1993, Tectonic and diagenetically induced seal failure within the south-western Great Bahamas Bank: Marine and Petroleum Geology, v. 10, p. 14–28, https://doi.org/10.1016/0264-8172(93)90096-B.

Whitaker, C.R., 1974, Plunge pool: The Australian Geographer, v. 12, no. 5, p. 459–461, https://doi.org/10.1080/00049187408702659.

Woods Hole Oceanographic Institution (WHOI), 2003, Multibeam collection for AT07L30: Multibeam data collected aboard Atlantis from 04-Mar-03 to 12-Mar-03, Jacksonville, Florida to Nassau, Bahamas: NOAA National Centers for Environmental Information, https://www.ngdc.noaa.gov/ships/atlantis/AT07L30_mb.html (accessed 16 January 2018).

Woods Hole Oceanographic Institution (WHOI), 2005, Multibeam collection for KN182L02: Multibeam data collected aboard Knorr from 02-May-05 to 26-May-05, St. George's, Bermuda to Miami, Florida: NOAA National Centers for Environmental Information, https://www.ngdc.noaa.gov/ships/knorr/KN182L02_mb.html (accessed 16 January 2018).

Zhang, K., Guan, Y., Song, H., Fan, W., Li, H., Kuang, Y., and Geng, M., 2020, A preliminary study on morphology and genesis of giant and mega pockmarks near Andu Seamount, Nansha Region, South China Sea): Marine Geophysical Researches, v. 41, no. 1, https://doi.org/10.1007/s11001-020-09404-y.

Science Editor: Wenjiao Xiao
Associate Editor: Jeff Hannon

Manuscript Received 8 April 2021
Revised Manuscript Received 25 February 2022
Manuscript Accepted 23 April 2022

Printed in the USA